Contribution from the Department of Chemistry,
McMaster University, Hamilton, Ontario L8S 4M1, Canada

Properties of Atoms in Molecules: Krypton and Xenon and Their Bonds to Nitrogen and Fluorine in $HC{\equiv}N{-}NgF^+$, NgF^+, and NgF_2

Preston J. MacDougall,† Gary J. Schrobilgen, and Richard F. W. Bader*

Received August 17, 1988

The recent synthesis of a salt of $FKr{-}NCH^+$, together with the earlier preparation of its Xe analogue, makes possible a comparison of the experimental properties of the bonds formed by N and F to the noble-gas atoms (Ng) Kr and Xe. This experimental study is complemented by a theoretical investigation at the SCF level of the properties of molecules containing such bonds and by the determination of the properties of the atoms and bonds in these molecules using the theory of atoms in molecules. The exceptional ability of the NgF^+ ions to act as Lewis acids is related to the presence of holes in the valence shell charge concentrations of the Kr and Xe atoms that expose their cores. The mechanism of formation of the Ng–N bonds in the adducts of NgF^+ with HCN is similar to the formation of a hydrogen bond: the mutual penetration of the outer diffuse nonbonded densities of the Ng and N atoms is facilitated by their dipolar and quadrupolar polarizations, which remove density from along their axis of approach, to yield a final density in the interatomic surface that is only slightly greater than the sum of the unperturbed densities. The Ng–N interactions lie closer to the closed-shell limit than do the Ng–F bonds formed in the reaction of NgF^+ with F^-. The energies of formation of these adducts are dominated by the large stabilizations of the Ng atoms that result from the increase in the concentration of charge in their inner quantum shells.

Introduction

The compound $FKr{-}N{\equiv}CH^+AsF_6^-$, the first to contain a krypton–nitrogen bond, was recently synthesized at this university.[1] Prior to this, the only known compounds of krypton were the Kr–F bonded species KrF_2, KrF^+, and $Kr_2F_3^+$ [2a] as well as $KrF_2{\cdot}WOF_4$ and $KrF_2{\cdot}n(MoOF)_4$ (n = 1–3).[2b] The corresponding compound containing a Xe–N bond was synthesized earlier[3] through the reaction of $XeF^+AsF_6^-$ or $Xe_2F_3^+AsF_6^-$ with HCN. The krypton compound was not prepared in such a direct manner because KrF^+ is too strong an oxidizing agent. Instead, its synthesis was obtained by allowing KrF^+ to react with the protonated HCN salt $HCNH^+AsF_6^-$. The Xe compound, $FXe{-}N{\equiv}CH^+AsF_6^-$, is stable up to −10 °C while the corresponding limit for the Kr compound is around −50 °C. It is the purpose of this paper to compare the properties of the bonds formed by F and N to Kr and Xe in terms of their experimental properties and by use of the theory of atoms in molecules.[4–6]

Energies and Geometries

Single determinantal SCF calculations with linearly constrained geometry optimizations using the program GAMESS[7] were performed for ArF^+, KrF^+, XeF^+, KrF_2, XeF_2, $FKrNCH^+$, and $FXeNCH^+$. Huzinaga's basis sets for Kr (432121s/42121p/311d) and Xe (4332121s/432121p/4211d)[8] were employed while the other atoms were described by the 4-31G** basis[9] augmented with diffuse s and p functions.[10] Previous ab initio calculations on the diatomic NgF^+ species have been performed by Liebman and Allen (HeF^+, NeF^+, and ArF^+),[11,12] Liu and Schaefer (KrF^+),[13] Frenking et al. (HeF^+, NeF^+, and ArF^+),[14] and Hottoka et al. (NeF^+).[15] Basch et al.[16] have included XeF_2 in a theoretical study of the neutral fluorides of xenon while Bagus et al.[17] have performed a CI calculation for a portion of the potential energy surface for KrF_2.

The minimum energy geometrical parameters and the total energies obtained here are given in Table I. The energies of the reaction between the closed-shell species HCN and FNg^+

$$FNg^+ + NCH \rightarrow FNg{-}NCH^+ \qquad (1)$$

are calculated to be −32.5 and −34.5 kcal/mol for Ng = Kr and Xe, respectively, while the corresponding energies of the ion reaction

$$FNg^+ + F^- \rightarrow F{-}Ng{-}F \qquad (2)$$

are −209.0 and −211.9 kcal/mol.

In spite of a lack of relativistic corrections, which tend to reduce the predicted bond distances to a heavy atom,[18] the calculated bond lengths for the two difluorides are in good agreement with the experimental results, with errors typical of SCF calculations

Table I. Energies and Geometries of Ng Compounds[a]

species	energy, au	calcd (exptl) bond lengths, Å
ArF^+	−624.97477	1.628
KrF^+	−2848.47027	1.734
XeF^+	−7325.92011	1.886
KrF_2	−2948.13396	1.843 (1.875 ± 0.002)[b]
XeF_2	−7425.58845	1.985 (1.977 ± 0.0015)[c]
$FKrNCH^+$	−2941.31362	1.748 [Kr–F], 2.307 [Kr–N], 1.128 [N–C], 1.068 [C–H]
$FXeNCH^+$	−7418.76656	1.904 [Xe–F], 2.421 [Xe–N], 1.127 [N–Cl], 1.068 [C–H]
HCN	−92.79150	1.132 (1.156) [C–N], 1.060 (1.064) [C–H][d]
F^-	−99.33059	

[a] See text for basis sets. [b] Murchison, C.; Reichman, S.; Anderson, D.; Overend, J.; Schreiner, F. *J. Am. Chem. Soc.* **1968**, *90*, 5690. Gas-phase infrared data. [c] Agron, P. A.; Begun, G. M.; Levy, H. A.; Mason, A. A.; Jones, G.; Smith, D. F.; *Science* **1963**, *139*, 842. Smith, D. F. *J. Chem. Phys.* **1963**, *38*, 270. Gas-phase infrared data. [d] Herzberg, G. *Electronic Spectra of Polyatomic Molecules*; Van Nostrand: New York, 1966.

† Present address: Department of Chemistry, Texas A&M University, College Station, TX 77843.

(1) Schrobilgen, G. J. *J. Chem. Soc., Chem. Commun.* **1988**, 863.
(2) (a) Gillespie, R. J.; Schrobilgen, G. J. *Inorg. Chem.* **1976**, *15*, 22. (b) Holloway, J. H.; Schrobilgen, G. J. *Inorg. Chem.* **1981**, *20*, 3363.
(3) Emara, A. A. A.; Schrobilgen, G. J. *J. Chem. Soc., Chem. Commun.* **1987**, 1644.
(4) Bader, R. F. W.; Beddall, P. M. *J. Chem. Phys.* **1972**, *56*, 3320.
(5) Bader, R. F. W.; Nguyen-Dang, T. T. *Adv. Quantum Chem.* **1981**, *14*, 63.
(6) Bader, R. F. W.; Nguyen-Dang, T. T.; Tal, Y. *Rep. Prog. Phys.* **1981**, *44*, 893. Srebrenik, S.; Bader, R. F. W. *J. Chem. Phys.* **1975**, *63*, 3945.
(7) Dupius, M.; Spangler, D.; Wendoloski, J. J. *NRCC Software Catalog* **1980**, *1*, QG01.
(8) Huzinaga, S. *Gaussian Basis Sets for Molecular Calculations*; Elsevier: Amsterdam Publ. 1984.
(9) Hehre, W. J.; Ditchfield, R.; Pople, J. A. *J. Chem. Phys.* **1972**, *56*, 2257.
(10) Chandrasekar, J.; Andrade, J. G.; Schleyer, P. v. R. *J. Am. Chem. Soc.* **1981**, *103*, 5609.
(11) Liebman, J. F.; Allen, L. C. *J. Am. Chem. Soc.* **1970**, *92*, 3539.
(12) Liebman, J. F.; Allen, L. C. *J. Chem. Soc., Chem. Commun.* **1969**, 1355.
(13) Liu, B.; Schaefer, H. F. *J. Chem. Phys.* **1971**, *55*, 2369.
(14) Frenking, G.; Koch, W.; Deakyne, A.; Liebman, J. F.; Bartlett, N., in press.
(15) Hottoka, M.; Roos, B.; Delos, J. B.; Srivastava, R.; Sharma, R. B.; Koski, W. S. *Phys. Rev. A* **1987**, *45*, 4515.
(16) Basch, H.; Moskowitz, J. W.; Hollister, C.; Hankin, D. *J. Chem. Phys.* **1971**, *55*, 1922.
(17) Bagus, P. S.; Liu, B.; Schaefer, H. F. *J. Am. Chem. Soc.* **1972**, *94*, 6635.

0020-1669/89/1328-0763$01.50/0

Table II. Correlation of Physical Properties for Representative Ng–F Bonds

species[a]	r(Ng–F),[b] Å	ν(Ng–F), cm^{-1}	NMR params[c] $^1J(^{129}Xe-^{19}F)$,[d] Hz	$\delta(^{129}Xe)$,[d,e] ppm	$\delta(^{19}F)$,[d,e] ppm	T, °C	ref
KrF^+	(1.740)						
$KrF^+Sb_2F_{11}^-$		624					*l*
$KrF^+AsF_6^-$		609					*l*, *m*
$(FKr)_2F^+$[f]		605			73.6	−65	*l*
$HC{\equiv}N{-}KrF^+$	(1.748)	560			99.4	−57	*n*
$CF_3C{\equiv}N{-}KrF^+$					93.1	−59	*o–q*
KrF_2	1.875	462			68.0	−56	*p*, *q*
	(1.843)						
XeF^+	(1.886)						
$XeF^+Sb_2F_{11}^-$	1.82 (3)	619	7230	−574	−290.2	23[g]	*l*, *r–t*
$XeF^+AsF_6^-$	1.873 (6)	610	6892	−869		−47	*l*, *m*, *o*, *u*
$(FXe)_2F^+$[f]	1.90 (3)	593	6740	−1051	−252.0	−62	*l*, *s*, *t*, *v*
$CF_3C{\equiv}N{-}XeF^+$			6397	−1337	−210.4	−63	*o*
$HC{\equiv}N{-}XeF^+$	(1.904)	564	6181	−1569	−198.4[h]	−58	*w*
$CH_3C{\equiv}N{-}XeF^+$[h]		565	6020	−1708	−185.5	−10	*w*
s-$C_3F_3N_2N{-}XeF^+$		548	5932	−1862	−145.6	−50	*o*
$FO_2SO{-}XeF$	1.940 (8)	528	5830	−1666		−40	*s*, *t*, *x*, *y*
cis/*trans*-$F_4OIO{-}XeF$		527	5803/5910	−1824/−1720	−161.7/−170.1[l]	0	*z*
$C_5F_5N{-}XeF^+$		528	5926	−1922	−139.6	−30	*aa*
4-$CF_3C_5F_4N{-}XeF^+$		524	5977	−1853	−144.6	−50	*aa*
$F_5TeO{-}XeF$[j]		520		−2051	−151.0[k]	26	*bb*, *cc*
$(FO_2S)_2N{-}XeF$	1.967 (3)	506	5586	−1977	−126.1	−58	*dd*, *ee*
			5664[j]	−2009[j]	−126.0[j]	−40	
XeF_2	1.977	496	5621	−1685	−184.3	−52	*o*, *ff*, *gg*
	(1.984)						

[a] Unless otherwise indicated, all cations have AsF_6^- as the counterion. [b] Values in parentheses are calculated values determined in the present work. [c] Spectra were obtained in BrF_5 solvent unless otherwise indicated. [d] The NMR parameters of KrF and XeF groups are very sensitive to solvent and temperature conditions; it is therefore important to make comparisons in the same solvent medium at the same or nearly the same temperatures. [e] Referenced with respect to the neat liquids $XeOF_4$ (^{129}Xe) and $CFCl_3$ (^{19}F) at 24 °C; a positive sign denotes the chemical shift of the resonance in question occurs to high frequency of (is more deshielded than) the resonance of the reference substance. [f] Table entries refer to the terminal fluorine on the noble-gas atom. [g] Recorded in SbF_5 solvent. [h] $\delta(^{19}F)$ measured in anhydrous HF solvent at −10 °C. [i] $\delta(^{19}F)$ measured in SO_2ClF solvent at −40 °C. [j] NMR parameters measured in SO_2ClF solvent. [k] NMR parameter measured in SO_2ClF solvent at −50 °C. [l] Gillespie, R. J.; Schrobilgen, G. J. *Inorg. Chem.* **1976**, *15*, 22. [m] Schrobilgen, G. J. Unpublished work. [n] Schrobilgen, G. J. *J. Chem. Soc., Chem. Commun.* **1988**, 863. [o] Schrobilgen, G. J. *J. Chem. Soc., Chem. Commun.* **1988**, 1506. [p] Murchison, C.; Reichman, S.; Anderson, D.; Overend, J.; Schreiner, F. *J. Am. Chem. Soc.* **1968**, *90*, 5680. [q] Claassen, H. .; Goodman, G. L.; Malm, J. G.; Schreiner, F. *J. Chem. Phys.* **1965**, *42*, 1229. [r] Burgess, J.; et al. *J. Inorg. Nucl. Chem., Suppl.* **1976**, 183. [s] Schrobilgen, G. J.; Holloway, J. H.; Granger, P.; Brevard, C. *Inorg. Chem.* **1978**, *17*, 980. [t] Gillespie, R. J.; Netzer, A.; Schrobilgen, G. J. *Inorg. Chem.* **1974**, *13*, 1455. [u] Zalkin, A.; et al. *Inorg. Chem.* **1978**, *17*, 1318. [v] Bartlett, N.; et al. *Inorg. Chem.* **1974**, *12*, 780. [w] Emara, A. A. A.; Schrobilgen, G. J. *J. Chem. Soc. Chem. Commun.* **1987**, 1644. [x] Bartlett, N.; et al. *Inorg. Chem.* **1972**, *11*, 1124. [y] Landa, B.; Gillespie, R. J. *Inorg. Chem.* **1973**, *12*, 1383. [z] Syvret, R. G.; Schrobilgen, G. J. *Inorg. Chem.*, submitted for publication. [aa] Emara, A. A. A.; Schrobilgen, G. J. *J. Chem. Soc. Chem. Commun.* **1988**, 257. [bb] Birchall, T.; Myers, R. D.; deWaard, H.; Schrobilgen, G. J. *Inorg. Chem.* **1982**, *21*, 1068. [cc] Sanders, J. C. P.; Schrobilgen, G. J. Unpublished work. [dd] Sawyer, J. F.; Schrobilgen, G. J.; Sutherland, S. J. *Inorg. Chem.* **1982**, *21*, 4064. [ee] Schumacher, G. A.; Schrobilgen, G. J. *Inorg. Chem.* **1983**, *22*, 2178. [ff] Reichman, S.; Schreiner, F. *J. Chem. Phys.* **1969**, *51*, 2355. [gg] Agron, P. A.; Begun, G. M.; Levy, H. A.; Mason, A. A.; Jones, G.; Smith, D. F. *Science* **1963**, *139*, 842.

with extended basis sets, (compare the results for HCN). The reaction of the NgF^+ ions with F^- to yield the difluorides results in increases in the Ng–F bond lengths of 0.1 Å, while their reaction with HCN causes the same bonds to lengthen on average by only 0.016 Å. There is a correlation of Ng–F bond length, as is also reflected in its vibrational frequency, with the base strength of the ligand attached to Ng–F^+. This is illustrated by the examples shown in Table II. The NgF^+ species are only weakly coordinated by a fluorine bridge to the anion $Sb_2F_{11}^-$ while the interaction of NgF^+ with $N(SO_2F)_2^-$ is representative of a much stronger interaction. Thus as the strength of the base B increases and the Ng–B bond becomes progressively less ionic, the Ng–F bond is lengthened and weakened. The observed values of the Ng–F vibrational frequencies place the adducts with HCN toward the most ionic end of the scale. The same trends are reflected in the ^{19}F and ^{129}Xe chemical shifts, which are also listed in Table II, if one accepts the correlation of increased shielding (more negative chemical shift) with a transfer of charge to Xe and hence with a reduced ionic character of the Ng–B interaction.

Quadrupolar nuclei in noncubic environments generally yield poorly resolved one-bond coupling patterns in their NMR spectra due to quadrupolar relaxation effects. In spite of the axial symmetry of the FXe–NCH^+ cation the ^{14}N NMR spectrum showed well resolved and only partially quadrupole collapsed $^1J(^{129}Xe-^{14}N)$, $^1J(^{14}N)$, and $^1J(^{13}C)$ couplings.[3] The extent of minimal quadrupolar relaxation via a reduced electric field gradient was examined theoretically by calculating this field gradient at the nitrogen nucleus and comparing it to that in isolated HCN. The principal component of the electric field tradient tensor, $(\nabla E)_{zz}$ ($+z$ is in the direction H → N), at the position of the nitrogen nucleus decreases from +1.02 au in HCN to +0.49 au in FXe–NCH^+. The electric field gradient at the nitrogen nucleus is halved upon formation of the KrF^+ adduct as well; thus, it may be possible to observe highly resolved $^1J(^{14}N-^{13}C)$ coupling in the ^{14}N NMR of this adduct. As a further check of the accuracy of these calculations, we have calculated the electric field gradients at the Xe nucleus in XeF^+ and FXe–NCH^+ and find them to differ by less than 7%, a result in agreement with the experimental observation that the quadrupolar splitting observed in the ^{129}Xe Mössbauer spectra of FXe–NCH^+ (40.2 ± 0.3 mm/s) is, within experimental error, the same as that obtained for the salt $XeF^+AsF_6^-$ (40.5 ± 0.1 mm/s).[19]

The C–N bond of HCN is calculated to shorten by ≈0.05 Å on forming the adducts, while the C–H bond is calculated to lengthen by 0.008 Å. These predicted changes in bond length are in agreement with the observed shifts in their corresponding stretching frequencies, ν(CN) increasing by 70 cm^{-1} for both compounds and ν(C–H) decreasing by 171 cm^{-1} in the Xe adduct.[3]

(18) Ziegler, T.; Snijders, J. G.; Baerends, E. J. *J. Chem. Phys.* **1981**, *74*, 1271.

(19) Valsdóttir, J.; Frampton, C.; Birchall, T.; Schrobilgen, G. J. Unpublished results.

Table III. Bond Properties of HCN and of Ng Compounds (in au)

bond A–B	R	r_b(A)	r_b(B)	ρ_b	$\nabla^2\rho_b$	λ_1	$\lambda_\perp$	Δr(Ng)	Δr(N)	$\rho_b{}^a$
H–CN	2.002	0.681	1.321	0.302	−1.334	0.394	−0.864			
HC–N	2.138	0.734	1.404	0.497	+0.891	3.067	−1.088			
FKr–NCH$^+$	4.359	2.171	2.188	0.053	+0.169	0.268	−0.050	1.26	1.39	0.047
FXe–NCH$^+$	4.575	2.318	2.257	0.049	+0.150	0.224	−0.037	1.40	1.32	0.046
F–F	2.538	1.269	1.269	0.332	+0.353	2.209	−0.928			
Ar–F$^+$	3.076	1.612	1.464	0.266	+0.136	0.982	−0.423			
Kr–F$^+$	3.277	1.664	1.624	0.184	+0.134	0.664	−0.265			
Xe–F$^+$	3.565	1.813	1.752	0.141	+0.312	0.648	−0.168			
F–KrF	3.483	1.755	1.728	0.138	+0.274	0.619	−0.173			
F–XeF	3.752	1.847	1.905	0.109	+0.314	0.541	−0.114			

Table IV. Properties of Atoms in Ng–F$^+$ and HCN

atom Ω	$q(\Omega)$	$\mu(\Omega)^a$	$Q_{zz}(\Omega)$	atom Ω	$q(\Omega)$	$\mu(\Omega)^a$	$Q_{zz}(\Omega)$
Ar	+0.928	+0.257	3.262	F	+0.072	−0.063	1.520
Kr	+1.148	+0.465	5.185	F	−0.148	+0.050	1.219
Xe	+1.406	+0.883	8.496	F	−0.406	+0.160	0.940
H	+0.193	+0.098	0.376	C	+1.260	+1.135	2.238
N	−1.454	+0.958	0.060				

[a] When $\mu(\Omega) > 0$, the negative end of the dipole is directed away from F and toward Ng or away from N and toward H.

Table V. Changes in Atomic Properties in Formation of FNg–NCH$^+$ and FNg–F ($\Delta E(\Omega)$ in kcal/mol; Other Properties in au)

	F	Kr	N	C	H
$\Delta q(\Omega)$	−0.169	+0.026	−0.102	+0.123	+0.123
$\Delta\mu(\Omega)$	−0.003	−0.075	+0.087	+0.083	−0.002
$\Delta Q_{zz}(\Omega)$	−0.143	+1.018	+0.471	−0.953	−0.091
	F	Xe	N	C	H
$\Delta q(\Omega)$	−0.132	+0.009	−0.133	+0.128	+0.128
$\Delta\mu(\Omega)$	−0.017	−0.246	+0.041	+0.088	−0.002
$\Delta Q_{zz}(\Omega)$	−0.091	+1.771	+0.330	−0.994	−0.094
	F[a]	Kr	F[a]	Xe	
$\Delta q(\Omega)$	−0.434	+0.016	−0.291	−0.012	
$\Delta\mu(\Omega)$	−0.035	−0.883	−0.088	−0.465	
$\Delta Q_{zz}(\Omega)$	−0.282	+2.085	−0.164	+3.511	
$\Delta E(\Omega)$	−129.2 (+98.8)	−178.6	−76.1 (+23.5)	−159.4	

[a] The energy differences in parentheses are calculated relative to the energy of F^-; the remaining values in these columns are calculated relative to the values for the F atoms in NgF^+.

These experimental characterizations of the bonds are complemented with the theoretical results obtained from an investigation of the charge distributions and properties of the atoms in the reactants and the changes they undergo on forming the adducts.

Atoms and Bonds

The necessary and sufficient condition for two atoms to be bonded to one another is that their nuclei be joined by an atomic interaction line in an equilibrium geometry, i.e., that they be linked by a bond path.[20,21] The presence of such a path indicates that electronic charge has been accumulated between the nuclei in an absolute sense, for it denotes the presence of a line linking the nuclei along which the charge density is a maximum with respect to any neighboring line.[22,23] The charge distributions of the complexes exhibit such lines between the Ng and N nuclei, as illustrated in Figure 1 for the Kr adduct. The presence of a bond path implies the existence of a bond critical point, the point along the bond path where the charge density ρ attains its minimum value and where $\nabla\rho = 0$. While the value of ρ is a minimum at

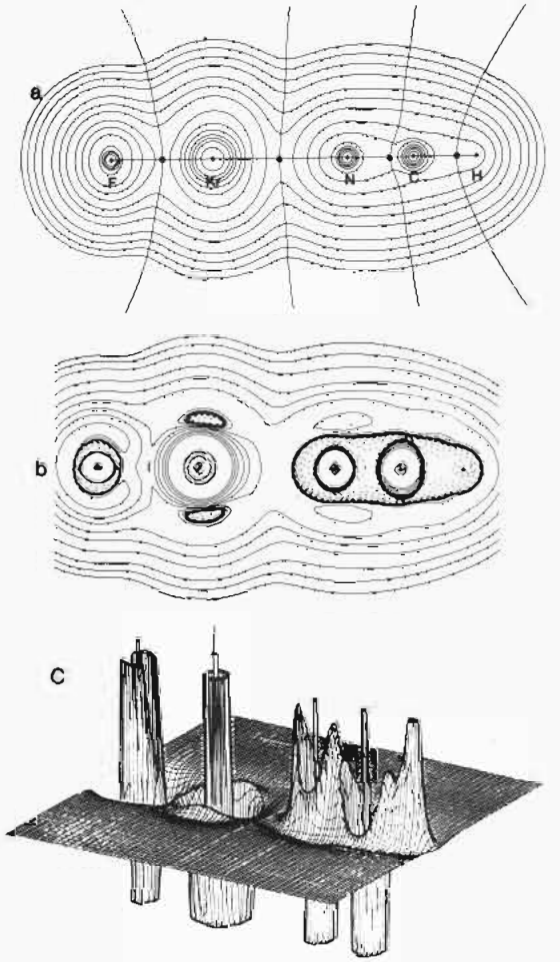

Figure 1. (a) Contour map of the charge density in the adduct FKrNCH$^+$ showing the bond paths and the intersection of the interatomic surfaces. Bond critical points are denoted by black circles. Note the near planarity of the Kr–N interatomic surface, which is also a characteristic of a hydrogen bond. The outer contour value is 0.001 au. The remaining contours increase in value in the order 2×10^n, 4×10^n, 8×10^n with n starting at −3 and increasing in steps of 1 to give a maximum contour value of 20. (b) Contour map of the Laplacian distribution for FKrNCH$^+$. The positions of the nuclei are the same as in part a. Solid contours denote positive and dashed lines denote negative values of $\nabla^2\rho$. The magnitudes of the contour values are as in part a, without the initial value of 0.001 au. (c) A relief map of $-\nabla^2\rho$. A maximum in the relief map is a maximum in charge concentration. If the inner spikelike feature at its nucleus is counted, the Kr atom exhibits four alternating regions of charge concentration and charge depletion corresponding to the presence of four quantum shells. Note the absence of a lip on the N side of the Kr VSCC demonstrating the presence of a hole in its outer sphere of charge concentration. Contrast the localized, atomic-like nature of the Laplacian distribution for the F and Kr atoms with the continuous valence shell of charge concentration enveloping all three of the nuclei in HCN.

(20) Bader, R. F. W.; Essén, H. *J. Chem. Phys.* **1984**, *80*, 1943.
(21) Bader, R. F. W. *Acc. Chem. Res.* **1985**, *18*, 9.
(22) Bader, R. F. W. In *International Review of Science: Physical Chemistry, Series 2*; Buckingham, A. D., Coulson, C. A., Eds.; Butterworths: London, 1975; Vol. 1. Runtz, G.; Bader, R. F. W.; Messer, R. R. *Can. J. Chem.* **1977**, *55*, 3040.
(23) The presence of a line of maximum charge density linking bonded nuclei and its absence when no bond is present is graphically illustrated for the bridgehead carbon atoms in propellanes and their corresponding bicyclic analogues: Wiberg, K. B.; Bader, R. F. W.; Lau, C. D. H. *J. Am. Chem. Soc.* **1987**, *109*, 985.

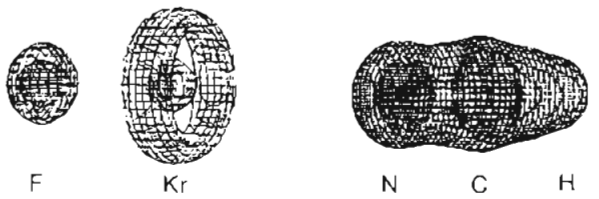

Figure 2. Zero envelopes of the Laplacian distributions ($\nabla^2\rho = 0$ for all points on the surface) for isolated KrF^+ and HCN shown aligned for adduct formation and shown to the same scale. The separation between the Kr and N nuclei is 5.0 Å. All that remains of the VSCC of the Kr atom is a belt of charge concentration, and the diagram clearly illustrates the exposure of its penultimate spherical shell of charge concentration—the core of the krypton atom. The diagram also contrasts the interatomic nature of the charge concentration in HCN with its pronounced intraatomic form in KrF^+.

this point along the bond path, it is a maximum with respect to directions perpendicular to this path. The lines of steepest descent through the three-dimensional charge distribution starting from the bond critical point define the interatomic surface (Figure 1). Such a surface is not crossed by any vectors $\nabla\rho$—it is a "zero flux surface".[4] These surfaces partition the space of a molecule into atoms, and the properties of each atom, because this space is a region of space bounded by a zero flux surface, are defined and predicted by quantum mechanics.[5,24] The bonds in the reactants and adducts are classified in terms of the properties of the charge density at the bond critical points (Table III). The formation of the adducts is discussed in terms of the properties of the atoms and their changes, Tables IV and V. Values of properties evaluated at a bond critical point are denoted by the subscript b. It has been shown[25] that in general, the properties of ρ at the bond critical points and its integrated averages over an atomic basin are relatively insensitive to electron correlation, the SCF values differing by small percentages relative to results obtained in CI calculations. The addition of correlation does not alter the classification of the bonds obtained by using SCF densities.

Bond Classification

The Laplacian of the charge density has the important property of determining where electronic charge is locally concentrated ($\nabla^2\rho < 0$) and locally depleted ($\nabla^2\rho > 0$),[20] information which is not evident in the topology of ρ itself. The local maxima in the concentrations of charge defined in this manner recover the Lewis model of localized electron pairs and the associated VSEPR model of molecular geometry,[26,27] while the course of a generalized Lewis acid–base reaction is predicted by aligning a maximum of charge concentration on the base with a minimum corresponding to a region of charge depletion on the acid.[26,28-30] The Laplacian distributions of the acids NgF^+ and the base HCN correctly predict the formation of the adducts described here. This is dramatically illustrated in Figure 2 where the plots of the zero envelope of $\nabla^2\rho$, which separates the valence shell of charge concentration (VSCC) from the valence shell of charge depletion, demonstrates the presence of a charge concentration (a maximum in $-\nabla^2\rho$) corresponding to the nonbonded electron pair on N of HCN and an axial hole in the valence shell of charge concentration of the Kr atom of KrF^+. The alignment of the maximum in charge concentration of the base with the hole in the VSCC of the acid yields the linear adduct.

Frontier orbital theory describes the formation of these adducts in terms of the overlap of the HOMO, corresponding to the nonbonded σ orbital localized on N, with the LUMO of the acid, the antibonding σ orbital localized on Ng. There is frequently a correspondence of HOMO and LUMO with the charge concentration in the VSCC of the base and the hole in the VSCC of the acid, respectively,[28,31] as is again evident in the present examples. The LUMO's of both KrF^+ and XeF^+ have negative orbital energies ($\approx$−6.0 eV), a reflection of the strong acidic character of these ions. This same behavior is reflected by the presence of actual holes in the VSCC's of Kr and Xe in these molecular ions, which provide a base with direct access to the inner cores of these atoms. There is a sphere in the VSCC of a free Ng atom over which the electronic charge is maximally concentrated (the radial curvature of $-\nabla^2\rho$ is negative over the entire sphere). Usually upon chemical combination this sphere persists but is no longer uniform, as local maxima and minima are created on its surface. In the case of strong Lewis acids such as BH_3 and carbonium ions, however, this sphere of charge concentration is punctured and reduced to a beltlike structure as found here for Kr and Xe in NgF^+. In ArF^+, however, the sphere of charge concentration persists and $\nabla^2\rho$ is negative over the whole of its VSCC. This qualitative difference with KrF^+ and XeF^+ is reflected in the barely negative LUMO energy of ArF^+, −0.6 eV. Thus the properties of the Laplacian distributions for these compounds, in addition to predicting the formation of the linear adducts, show the Kr and Xe molecular ions to be stronger Lewis acids than is ArF^+. This conclusion lends credence to the calculations of Frenking et al.,[14] which indicate that $ArF^+AuF_6^-$ should possess at least marginal stability in the solid state.

If $\nabla^2\rho(\mathbf{r}) < 0$, then the value of ρ at the point r is greater than the value of ρ averaged over an infinitesimal sphere centered at r. The corresponding statement is true in one dimension, and since the charge density is a minimum at the bond critical point along the bond path, the associated curvature of ρ_b, λ, is positive and electronic charge is locally depleted at this point with respect to neighboring points along the bond path. The charge density is, however, a maximum at the critical point in the interatomic surface, the two curvatures of ρ_b perpendicular to the bond path, $\lambda_\perp$, being negative. Thus electronic charge is locally concentrated at the critical point with respect to the interatomic surface. The formation of a chemical bond and an interatomic surface is, therefore, the result of a competition between the perpendicular contractions of the charge density toward the bond path that lead to a concentration of electronic charge between the nuclei along the bond path and the parallel contraction of ρ that leads to its separate concentration in the basins of the neighboring atoms. The value of the Laplacian at the bond critical point, $\nabla^2\rho_b$, equals the sum of the three curvatures, $\nabla^2\rho_b = 2\lambda_\perp + \lambda$, and its sign determines which of the two competing effects is dominant in the formation of a given bond. The bonds in the adducts described here cover the spectrum of possible behavior.

When $\nabla^2\rho_b < 0$ and is large in magnitude as for the H–C bond in HCN (Table III), the perpendicular contractions in ρ dominate the interaction and electronic charge is concentrated between the nuclei along the bond path (see Figures 1 and 2) as is also reflected in the relatively large value of ρ_b. The result is a sharing of electronic charge between the nuclei as is found in covalent or slightly polar bonds as in NO, for example. The Laplacian of the charge density appears in the local expression of the virial theorem

$$\frac{1}{4}\nabla^2\rho(\mathbf{r}) = 2G(\mathbf{r}) + V(\mathbf{r}) \qquad (3)$$

where $G(\mathbf{r})$, which is always positive, is the kinetic energy density (it yields the electronic kinetic energy $T(\Omega)$ when integrated over the basin of atom Ω) and $V(\mathbf{r})$, which is always negative, is the potential energy density (it yields the electronic potential energy $V(\Omega)$ when integrated over the basin of the atom). Because of the zero flux surface condition, the integration of the Laplacian over an atom vanishes and thus integration of eq 3 yields the virial theorem $(2T(\Omega) + V(\Omega) = 0)$ for an atom, free or bound. The

(24) Bader, R. F. W. *Pure Appl. Chem.* **1988**, *60*, 145.
(25) Gatti, C.; MacDougall, P. J.; Bader, R. F. W. *J. Chem. Phys.* **1988**, *88*, 3792.
(26) Bader, R. F. W.; MacDougall, P. J.; Lau, C. D. H. *J. Am. Chem. Soc.* **1984**, *106*, 1594.
(27) Bader, R. F. W.; Gillespie, R. J.; MacDougall, P. J. *J. Am. Chem. Soc.* **1988**, *110*, 7329.
(28) Bader, R. F. W.; MacDougall, P. J. *J. Am. Chem. Soc.* **1985**, *107*, 6788.
(29) Carroll, M. T.; Chang, C.; Bader, R. F. W. *Mol. Phys.* **1988**, *63*, 387.
(30) Bader, R. F. W.; Chang, C. *J. Phys. Chem.*, in press.
(31) Tang, T.-H.; Bader, R. F. W.; MacDougall, P. J. *Inorg. Chem.* **1985**, *24*, 2047.

total energy density is given by $E(\mathbf{r}) = G(\mathbf{r}) + V(\mathbf{r})$,[5] and one has another form of the virial theorem, $E(\Omega) = -T(\Omega)$. As a consequence of eq 3, it follows that the total energy density is most negative (most stabilizing) in those regions of space where $\nabla^2\rho < 0$, that is, where electronic charge is concentrated and the potential energy density dominates the local virial relationship. Thus in a shared interaction, the atoms are bound because of the lowering of the potential energy associated with the charge concentration and shared between the nuclei.

In a very polar bond such as CN of HCN, the perpendicular contractions of ρ, as measured by $\lambda_\perp$, are greater than those for the H–C bond and electronic charge is concentrated between the nuclei to an even greater extent, as demonstrated by the Laplacian distribution in Figure 1 and as reflected in a larger value of ρ_b. However, the electronic charge is unequally shared between the atoms and as a result, the bond critical point is shifted toward the carbon core where the density rises very rapidly and the Laplacian undergoes a change in sign. At the critical point its sign is dominated by $\lambda_\parallel$ in spite of large negative values for $\lambda_\perp$.

These bond characteristics change little on formation of the adducts: ρ_b for C–H remains unchanged and $\nabla^2\rho_b$ decreases by 0.12 au while both quantities decrease by approximately 0.006 au for the C–N bond.

When $\nabla^2\rho_b > 0$ and ρ_b is small in value, one has the other extreme of bonding, one dominated by the contraction of each atomic density toward its own nucleus resulting in a depletion of charge at the critical point and in the interatomic surface. These are called closed-shell interactions as they typify interactions between closed-shell atoms as found in noble-gas repulsive states, ionic bonds, hydrogen bonds, and van der Waals molecules and in the relatively long bonds formed between what are formally closed-shell atoms, as between S atoms in S_4N_4 and S_8^{2+}.[20,29,31] The depletion of electronic charge in the interatomic surface arises because of the demands of the Pauli principle, and hence these interactions are typified both by a positive value for $\nabla^2\rho_b$ *and* a low value for ρ_b. In closed-shell interactions the charge concentrations and the associated lowering of the potential energy are separately localized in the basins of each of the atoms.

Reference to Figures 1 and 2 shows that the valence shells of all three atoms in the HCN fragment form one contiguous region of charge concentration—the valence shells of charge concentration (VSCC) are linked together over the H–C and C–N bonds as is typical of shared interactions, polar and nonpolar. For the Ng–N bonds and also for the Ng–F bonds, however, the VSCC's of the individual atoms are not linked. Instead charge is concentrated separately in each atomic basin and there is no shared concentration of charge. The Ng–N bonds result from the interaction of the closed-shell reactants NgF^+ and NCH, and they are examples of the closed-shell type of interaction. The values of ρ_b are small, the same order as found in ionic systems such as KF and NaCl, and $\nabla^2\rho_b$ is positive with $\lambda_\parallel \gg \lambda_\perp$, and both components are relatively small in magnitude (Table III). The mechanism of formation of the relatively long adduct bond Ng–N is similar to the formation of a hydrogen bond.

A hydrogen bond results from a partial penetration of the van der Waals envelope of the H atom of the acid and the base atom B of the base molecule, the strength of the interaction increasing with the degree of mutual penetration. Electronic charge is not concentrated in the interatomic surface as is typical of a shared interaction. Instead, the densities of the H and B atoms are polarized so as to remove density along their line of approach to facilitate the penetration of their nonbonded envelopes with the result that the final density at the H–B bond critical point is approximately equal to the sum of the unperturbed densities of the H and B atoms at their points of penetration.[32] These same features characterize the redistribution of charge found to accompany the formation of the Ng–N bonds.

A bonded radius of an atom is defined as the distance from its nucleus to the appropriate bond critical point and is denoted by $r_b(\Omega)$ (Table III). Its nonbonded radius is correspondingly defined as the distance from the nucleus to some outer contour of the charge density, $r_n(\Omega)$.[33,34] The contour shown in Figure 1 and used in the determination of the nonbonded radii, the 0.001 au contour, yields molecular sizes and atomic diameters in good agreement with gas-phase van der Waals radii.[33,35] The bonded radii for the Ng–N bonds are considerably greater than those for the other reactant bonds, including the Ng–F bonds. They result from the partial penetration of the outer van der Waals envelopes of the Ng and N atoms. The extent of this penetration is given by the difference between the nonbonded radii of the Kr, Xe, and N atoms in the reactants, $r_n(\Omega)$ equaling 3.43, 3.72, and 3.58 au, respectively, and the corresponding bonded radii of the Ng–N bonds (Table III). These changes in radii are given in Table III. The strength of a hydrogen bond in general parallels the degree of penetration of the van der Waals envelopes.[32] The total penetrations are 2.65 and 2.72 au for the Kr and Xe adducts, respectively. The greater penetration of the Xe atom and its greater total value are in agreement with its slightly greater energy of formation. The total penetration of 1.80 au encountered in the formation of the hydrogen-bonded complex FH–NCH is considerably less, as is its energy of formation of ≈6 kcal/mol. Also listed in Table III under ρ_b° is the sum of the values of the unperturbed densities of the isolated reactants at their points of penetration, i.e., at the positions determined by the values of the bonded radii in the adducts. It is a characteristic of bonds resulting from the penetration of closed-shell distributions that the value of ρ at the bond critical point differs little in value from the sum of the unperturbed reactant densities evaluated at the point of penetration, like the average value of 0.005 au found here. (The value of ρ_b° is 0.0177 au for the hydrogen bond in FH–NCH compared to a value of 0.0183 au for ρ_b.)

This analysis yields a picture of adduct or hydrogen-bond formation that corresponds to the mutual penetration of the outer diffuse nonbonded densities of the appropriate atoms of the base and acid molecules, with the final density at the bond critical point being only slightly greater than the sum of the unperturbed densities. Unlike a shared or covalent interaction, there is no concentration of charge density in the interatomic surface and along the bond path. The final density is instead determined primarily by the extent of penetration—the greater the penetration the larger the value of ρ_b and the stronger the resulting bond. The analysis of the atomic properties given below shows that both the Ng and N atoms of the reactants polarize in such a way as to facilitate this mutual penetration of their closed-shell density distributions.

The Ng–F bonds in the reactants NgF^+, including ArF^+ for an extended comparison, are intermediate between the two extremes of bonding and are similar in their characteristics to the bond in the isoelectronic F_2 molecule (Table III). This is particularly true for the first member of the series ArF^+ in which the valence electrons are nearly equally shared between the two atoms (Table IV), the net charge on Ar being close to +1. The net charge of atom Ω, $q(\Omega)$, is defined as the difference between its nuclear charge and its average number of electrons, $N(\Omega)$, the latter being obtained by an integration of the charge density over the basin of the atom.

$$q(\Omega) = Z_\Omega - N(\Omega) = Z_\Omega - \int_\Omega \rho(\mathbf{r})\, d\tau \qquad (4)$$

The positive charge on the Ng atom increases in the order Ar < Kr < Xe, and their bond characteristics exhibit a corresponding shift toward the closed-shell limit. While the charge density is contracted toward the bond path, leading to a significant value for ρ_b for F_2 and ArF^+, the interactions are increasingly dominated through the series by the separate localization of electronic charge in the basins of each of the atoms. Not only do the F and Ng

(32) Carroll, M. T.; Bader, R. F. W. *Mol. Phys.* **1988**, *65*, 695.
(33) Bader, R. F. W.; Henneker, W. H.; Cade, P. E. *J. Chem. Phys.* **1967**, *46*, 3341.
(34) Bader, R. F. W.; Beddall, P. M.; Cade, P. E. *J. Am. Chem. Soc.* **1971**, *93*, 3095.
(35) Bader, R. F. W.; Carroll, M. T.; Cheeseman, J. R.; Chang, C. *J. Am. Chem. Soc.* **1987**, *109*, 7968.

atoms bind their densities tightly but also the charge is physically localized within the boundaries of each atom.[20] Thus even in F_2 the intraatomic Fermi correlation is pronounced, the electrons are 93% localized within the basins of the separate atoms, compared to a value of 73% in a molecule such as C_2.[36] Such localization of charge, while providing the major source of binding in fluorides via a charge transfer to fluorine, is the antithesis of that required for the sharing of electronic charge through the mechanism of exchange as found in a homopolar bond such as F_2. Thus the bonds in F_2 and ArF^+ are relatively weak. This analysis leads one to conclude that the bond strengths should increase with the degree of charge transfer in the order $F_2 \approx ArF^+ < KrF^+ < XeF^+$. This conclusion is supported by the known dissociation energies, which in kcal/mol are 37.0,[37] ≥38, ≥36.4, and 46.8,[38] respectively. Liu and Schaefer[12] have calculated a value of 43.8 kcal/mol for KrF^+.

The Ng–F bonds of the molecular ions are only slightly perturbed on forming the adducts with HCN. Their bond lengths increase by 0.014 and 0.018 Å for Kr and Xe species, respectively, with corresponding small decreases in the values of ρ_b, of 0.005 and 0.008 au, and increases in the values of $\nabla^2\rho_b$ to 0.195 and 0.348 au. These changes are consistent with a weakening of the Ng–F bond and to a slight shift in its characteristics toward the closed-shell limit on formation of the adduct. There is a small shift in electronic charge from Ng to F (Table V). The same changes are found for the H–A bond of an acid in the formation of a hydrogen bond.

These same bonds (Ng–F) are perturbed to a much greater extent on the formation of the adducts with F^- and so is the shift toward the closed-shell limit of bonding in agreement with the experimental characterization of these bonds. The values of ρ_b and $\nabla^2\rho_b$ are decreased and increased, respectively. While the increase in the value of the Laplacian is quite small for the Xe adduct, the ratio of the parallel to the perpendicular contractions of ρ as measured by $\lambda_\parallel/\lambda_\perp$, increases significantly for both adducts from 2.5 to 3.6 and from 3.9 to 4.8 for the Kr and Xe compounds, respectively. Except for XeF_2, the Ng atoms are predicted to undergo small decreases in electron population on formation of the adducts. While this might appear to be at variance with the general conclusion that the Ng atom becomes more shielded as the base strength increases, as exemplified by ^{129}Xe chemical shift data given in Table II, this is not the case because small changes in population do not necessarily reflect corresponding changes in the screening of a nucleus. A more direct indicator of nuclear shielding is the quantity $V_{ao}(\Omega)$, the attraction of a nucleus for the electronic charge density in its own basin. An increase in the magnitude of this quantity, in spite of a loss of charge for the atom, implies that the density is more contracted toward the nucleus and hence is bound more tightly—and provides greater shielding. The magnitudes of $V_{ao}(Kr)$ relative to its value in KrF^+ are greater by 20.1 and 52.0 kcal/mol for the HCN and F^- adducts, respectively, in accord with the trend established in Table II. The properties of ρ at the bond critical point and of the atoms clearly indicate that the Ng–F bonds in the HCN adducts are intermediate in character between those for Ng–F^+ and for NgF_2.

Changes in Atomic Properties

In addition to the net charges on the atoms, Table IV lists the first and second moments of the atoms in the reactants and Table V gives the changes in the atomic properties on forming the adducts. The charge $q(\Omega)$ of atom Ω is defined in eq 4. The first moment $\mu(\Omega)$ measures the dipolar polarization of the atomic density and is defined as

$$\mu(\Omega) = -\int_\Omega \mathbf{r}_\Omega \rho(\mathbf{r})\, d\tau \qquad (5)$$

where the position vector $\mathbf{r}_\Omega$ is centered at the nucleus of atom Ω. The diagonal element of the quadrupole moment of an atomic distribution for the z axis is

$$Q_{zz}(\Omega) = -\int_\Omega \rho(\mathbf{r})\,(3z^2 - \mathbf{r}_\Omega^2)\, d\tau \qquad (6)$$

with corresponding definitions for the other diagonal elements. Each of the diagonal elements, which sum to zero, has the form of the familiar d_{z^2} orbital. For a spherical charge distribution, each equals zero. For the linear molecules considered here with z as the internuclear axis, $-{}^1/_2 Q_{zz}(\Omega) = Q_{xx}(\Omega) = Q_{yy}(\Omega)$. A positive value for $Q_{zz}(\Omega)$ implies that electronic charge is removed from along the internuclear axis and concentrated in a toruslike distribution about the axis. The quadrupole moment is the density complement of an orbital π population. Thus in acetylene, $Q_{zz}(C)$ is large and positive, equal to +4.14 au, corresponding to an accumulation of π density in a torus about the z axis. In benzene and ethylene, with z perpendicular to the plane of the nuclei, $Q_{zz}(C)$ is large and negative corresponding to the presence of one π electron per atom. The magnitude of $Q_{zz}(C)$ for the para carbon atom in substituted benzenes varies in a linear manner with its integrated π population,[30] from a maximum value in phenoxide ion to a minimum in nitrobenzene.

The charge on the Ng atom in NgF^+ increases from ≈+1 for Ar to +1.4 for Xe, and there is an accompanying increase in the polarizations of the density of the Ng atom away from the increasingly negatively charged F atom. It is a general result that atoms are polarized in a direction counter to the direction of charge transfer. Thus the N, C, and H atoms are all polarized in the direction N to H, because of the transfer of negative charge to N.

In forming a hydrogen bond AH–BX between an acid AH and a base BX, there is a small transfer of charge from the base to the acid. Within the acid itself, there is a still smaller loss of charge from H and a slightly larger gain in charge for the base atom B. There is thus a net transfer of charge from X to A. Both the H and B atoms polarize in such a way as to facilitate their mutual interpenetration: the polarization of H away from A is decreased, while the polarization of B toward X is increased. The quadrupolar polarizations of both H and B are increased, corresponding to a promotion of density from along the internuclear axis in their direction of approach to a torus of charge about the axis. This corresponds to a promotion of σ to π density. In the formation of FH–NCH, which has a relatively small energy of formation of ≈6 kcal/mol, the changes in populations of the acid atoms are $\Delta q(F) = -0.038$ and $\Delta q(H) = +0.021$ and in the atoms of the base are $\Delta q(N) = -0.039$ and $\Delta q(CH) = +0.056$, while the changes in quadrupole for the HCN fragment are $\Delta Q_{zz}(N) = 0.220$ au, $\Delta Q_{zz}(C) = -0.226$ au, and $\Delta Q_{zz}(H) = -0.017$ au.

Precisely the same changes in charge and polarizations accompany the formation of the rare-gas adducts, as can be seen from Table V. The F atom gains more electronic charge than the Ng atoms lose, and the N atom gains less electronic charge than the CH fragment loses. There is thus a net transfer of charge from the CH fragment to F as in the formation of a hydrogen bond. (The loss of charge from the CH fragment of the base is remarkably similar for the two adducts, as is the fact that both atoms lose the same amount of charge.) In both adducts the polarization of the Ng atoms away from F is decreased and the polarization of the N atom toward the CH fragment is increased. Finally, the value of $Q_{zz}(\Omega)$ is increased for both the Ng and N atoms and decreased for the remaining atoms, indicating that the dipolar and quadrupolar polarizations are such as to remove density from the Ng–N internuclear region and along their internuclear axis so as to facilitate the approach of two closed-shell systems.

These same polarizations are reflected in the changes of the Laplacian distributions upon adduct formation. The magnitude of the nonbonded charge concentration on the N atom is decreased from 3.4 au in HCN to 2.8 au in the adducts. The maximum magnitude attained in the vestigial belt of charge concentration in the VSCC's of the Ng atoms increases from 0.08 to 0.10 au for Kr and from 0.03 to 0.04 au for Xe, while the magnitude of the torroidal belt encompassing the axis on the N atom increases from 0.72 au in HCN to 0.89 au in the adducts. The same belt for the carbon atom, which loses π density on adduct formation[32]

(36) Bader, R. F. W.; Stephens, M. E. *J. Am. Chem. Soc.* **1975**, *97*, 7391.
(37) Darwent, B. de B. NBS Pub. NSRDS-NBS 31, 1970.
(38) Berkowitz, J.; Chupka, W. A. *Chem. Phys. Lett.* **1970**, *7*, 447.

and for which $\Delta Q_{zz}(C) < 0$, decreases in magnitude, from 0.72 au in HCN to 0.46 au in the adducts. Similar behavior is observed for the F atoms where the belt of charge concentration in its VSCC (see Figure 1) decreases in magnitude from 14.3 to 13.1 au for the Kr system, and from 12.9 to 11.8 for the Xe system.

The energy of an atom in a molecule is defined using the atomic statement of the virial theorem.[4,5,24] These theoretical energies agree with the experimentally measurable additive energies of the methyl and methylene groups in the saturated hydrocarbons,[39,40] thereby showing, together with their properties, that these atoms are the atoms of chemistry. Because the virial theorem is not satisfied to the same degree for HCN alone as it is for NgF^+ and their HCN adducts, the changes in the atomic energies cannot be discussed for reaction 1.[39] This difficulty is not encountered for the molecules involved in the formation of NgF_2, and the changes in the energies of the Ng and F atoms for reaction 2 are listed in Table V.

The energies of reaction 2 are dominated by the changes in the energies of the Ng atoms, and the same qualitative result is obtained for the formation of the HCN adducts. The considerable increase in stability of these atoms is not a result of charge-transfer effects, which are small and correspond to a slight loss in charge for Kr, but rather are a result of a reorganization of the charge within the Ng atoms and their interaction with the base atoms. As noted above, the charge density of the Kr atom in KrF^+ is contracted toward the nucleus in forming an adduct. In the case of KrF_2 this results in a contribution of 52 kcal/mol to the stabilization of the Kr atom, in spite of its loss of charge. This contraction is also evident in the change in the volume of the Kr atom on adduct formation, from 187 a_0^3 in KrF^+ to 169 a_0^3 in KrF_2.[41] Further stabilization results from the interaction of the density on the Ng atom with the nucleus of the base atom. These increased attractive interactions outweigh the increased destabilizing effects, the interatomic electron repulsions being minimized by the dipolar and quadrupolar polarizations of the densities of the Ng atoms as described above.

The considerable decrease in the energies of the Ng atoms on formation of a Lewis acid–base adduct is predicted by the theory of atoms in molecules is the quantum equivalent of the classical description of the interaction in terms of a large polarizable atom in the negative field of the base atom. The reason why the adducts of HCN with KrF^+ and XeF^+ are considerably more stable than the adduct formed with the acid HF are quantitatively accounted for by comparing the properties of the Ng atoms with those of H. The net positive charge on H is only 0.75 compared to 1.15 and 1.41 for Kr and Xe, respectively, in the three fluorides. The charge distribution of HF is dominated by the electronegative F, making the density on H difficult to polarize. The change in dipolar polarization of H on formation of FH–NCH is 0.02 au, 25–45 times smaller than that for the Ng atoms. The quadrupolar polarization of the H atom is similarly very slight, $\Delta Q_{zz}(H) =$ 0.07 au, compared to a promotion of axial to toroidal density corresponding to changes of 1.0–2.0 au in the $Q_{zz}(\Omega)$ values of the Ng atoms. The H of HF is a much "harder" atom than the Ng atoms, as is also reflected in the relatively small value of 0.79 au for the penetration of its van der Waals envelope in its reaction with HCN. As a result, the energy change for the H atom on hydrogen bond formation is small and, since it is dominated by a loss in charge, destabilizing.[32]

A comparison of the Laplacian distributions for the NgF^+ ions and HF[20] also show that the Kr and Xe atoms in NgF^+ are stronger Lewis acids than H of HF. The Laplacian distribution for HF[20] exhibits a single, continuous valence shell of charge concentration (VSCC) that encompasses the proton. There is a small local minimum in the valence shell of charge depletion located 0.72 au from the proton, as opposed to the presence of an actual hole in the VSCC of the Ng atoms, which, as discussed above and illustrated in Figures 1 and 2, lays bare to an approaching base the field of the central core of these atoms. Thus, in addition to the decrease in the magnitude of the nonbonded charge concentration on the nitrogen atom on adduct formation, there is an increase in the penultimate shell of charge concentration of the Ng atoms, corresponding to the third quantum shell in Kr (Figure 1) and to the fourth shell in Xe. These are the shells exposed by the holes in the valence shells of charge concentration in the Ng atoms (Figure 2). According to eq 3, which shows that the sign of the Laplacian determines the local departures of the kinetic and potential energy densities from their average ratio of 2:1, a Lewis acid–base reaction corresponds to the combination of a region with excess kinetic energy (the local charge depletion on the acid) with a region of excess potential energy (the local charge concentration on the base). It is the transfer of nonbonded charge from the VSCC on the N atom to the tightly bound inner quantum shell of charge concentration of the Kr or Xe atom as made possible by their dipolar and quadrupolar polarizations that results in the dramatic lowering in the energies of these atoms on adduct formation.

Acknowledgment is made to the donors of the Petroleum Research Fund, administered by the American Chemical Society, for partial support of this research (P.J.M. and R.F.W.B.). This research was also sponsored by the U.S. Air Force Astronautics Laboratory, Edwards Air Force Base, California, Contract 49620-87-C-0049 (G.J.S.), and a Natural Sciences and Engineering Research Council of Canada operating grant (G.J.S.).

Registry No. Kr, 7439-90-9; Xe, 7440-63-3; N_2, 7727-37-9; F_2, 7782-41-4; ArF^+, 11089-94-4; KrF^+, 11088-74-7; XeF^+, 47936-70-9; KrF_2, 13773-81-4; XeF_2, 13709-36-9; $FKrNCH^+$, 118494-40-9; $FXeNCH^+$, 118494-41-0; HCN, 74-90-8; F^-, 16984-48-8.

(39) Wiberg, K. B.; Bader, R. F. W.; Lau, C. D. H. *J. Am. Chem. Soc.* **1987**, *109*, 1001.
(40) Bader, R. F. W. *Can. J. Chem.* **1986**, *64*, 1036.
(41) The volume of an atom is a measure of the region of space enclosed by the union of the atom's interatomic surfaces and the 0.001 au density envelope.